Weirdest Martensite: Smectic Liquid Crystal Microstructure and Weyl-Poincaré Invariance

Danilo B. Liarte,[1,2,*] Matthew Bierbaum,[1] Ricardo A. Mosna,[3] Randall D. Kamien,[4] and James P. Sethna[1,†]
[1]Laboratory of Atomic and Solid State Physics, Cornell University, Ithaca, New York 14853-2501, USA
[2]Institute of Physics, University of São Paulo, São Paulo, São Paulo 05314-970, Brazil
[3]Departamento de Matemática Aplicada, Universidade Estadual de Campinas, Campinas, São Paulo 13083-859, Brazil
[4]Department of Physics and Astronomy, University of Pennsylvania, Philadelphia, Pennsylvania 19104, USA
(Received 6 November 2015; published 4 April 2016)

Smectic liquid crystals are remarkable, beautiful examples of materials microstructure, with ordered patterns of geometrically perfect ellipses and hyperbolas. The solution of the complex problem of filling three-dimensional space with domains of focal conics under constraining boundary conditions yields a set of strict rules, which are similar to the compatibility conditions in a martensitic crystal. Here we present the rules giving compatible conditions for the concentric circle domains found at two-dimensional smectic interfaces with planar boundary conditions. Using configurations generated by numerical simulations, we develop a clustering algorithm to decompose the planar boundaries into domains. The interfaces between different domains agree well with the smectic compatibility conditions. We also discuss generalizations of our approach to describe the full three-dimensional smectic domains, where the variant symmetry group is the Weyl-Poincaré group of Lorentz boosts, translations, rotations, and dilatations.

DOI: 10.1103/PhysRevLett.116.147802

The spatial decomposition of smectic liquid crystals into focal conic domains gives rise to one of the most unusual examples of materials microstructure. The smectic is a remarkable state of matter, breaking both the continuous rotational and (one-dimensional) translational symmetries of the isotropic fluid [1,2]. In the beginning of the twentieth century, Grandjean and Friedel inferred that smectics were lamellar materials based on their bizarre microstructure [3]; observe the beautiful patterns full of ellipses and hyperbolas in Fig. 1. The figure shows a two-dimensional planar boundary (the layer surfaces lying perpendicular to the section) of a simulated configuration of a 3D smectic A liquid crystal, mimicking experiments where thin slabs of smectic samples are placed between crossed polarizers [4] can be obtained by solving the equation $\boldsymbol{N} = \nabla\phi$ for ϕ, using Fourier methods. More information on our smectic visualizers can be found in our previous publication [5]. Friedel's breakthrough came with the realization that the visible conics could be modeled as the locus of the centers of curvature of a set of equally spaced layers. The smectic layers must bend into cyclides of Dupin, which are the general set of equally spaced surfaces whose singular centers of curvature lie along one-dimensional conics [6]. The smectic decomposes into the so-called focal conic domains (FCDs), which can be stabilized to mediate otherwise incompatible boundary conditions, such as anchoring of a sample boundary [7].

We propose here a theory of smectic microstructure that generalizes and merges the laws of association between domains first proposed by Friedel [8] and the mathematical theory of martensitic microstructure [9–12]. Our theory describes both the interpolation structure proposed by Beller *et al.* [13] to characterize the smectic flower textures, and Apollonius's packings in the FCD model of grain boundaries [7]. Smectic liquids form the world's weirdest martensite.

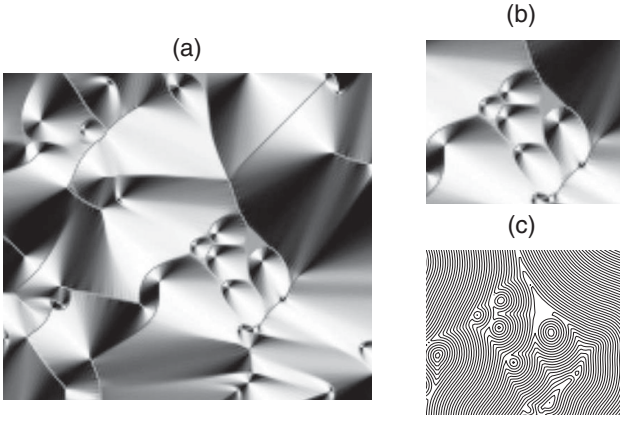

FIG. 1. (a) Crossed-polarizer images of focal conic domains on simulated smectics. (b) Elliptical defects attached to the upper surface (with planar boundary conditions). Note the hyperbolas emanating from the ellipses foci. Different focal conic domains (cyclides of Dupin) can rotate and deform via a Weyl-Poincaré transformation to join together compatibly continuous smectic layers. Note also the small gaps between the ellipses. It is energetically favorable to fill these regions with further ellipses, recursively down to molecular scales, leading to the "Apollonian packing" microstructure. (c) Layer sections forming concentric circles at the top boundary of the simulation.

 © 2016 American Physical Society

In a martensitic transformation, the phase transition between different crystal structures (for instance from cubic to tetragonal symmetry) yields a low-temperature phase where two or more discrete configurations with different shape anisotropy coexist [9]. This structure was discovered in c. 1890 by the microscopist Adolf Martens, though some of its mechanical properties have been used since (at least) the dawn of the Iron Age. Metallurgists and blacksmiths manipulate the martensitic microstructure (as well as the dislocation and precipitate structures) by heating and hammering swords and horseshoes to confer toughness and strength.

Martensites are usually characterized by a striped pattern, or laminate, that minimizes the constrained elastic free energy while keeping the net strain near zero. Figure 2 shows an example of a martensitic structure, with the dark and light regions representing two variants of the crystal martensite (see also SM discussion of paper folding as a martensite). The martensitic variants are akin to the smectic domains filled with a single family of Dupin cyclides.

In this paper, we generalize the mathematical theory of martensites in order to study the microstructure of smectic liquid crystals. We shall start by labeling the energy-minimizing states and variant symmetry groups of smectic and martensitic crystals. We then extract smectic configurations from planar boundaries of our simulations and apply a clustering algorithm to decompose two-dimensional space into domains where the layers form sets of concentric circles [Fig. 1(c)]. We finish by a discussion of some physical examples and open questions.

In a martensitic phase of a cubic to tetragonal transformation, we can describe the system by the vector field $\boldsymbol{y} = \boldsymbol{y}(\boldsymbol{x})$, where $\boldsymbol{x}$ and $\boldsymbol{y}$ are the positions of a point in reference and target spaces, respectively, and the reference space is associated with the austenite configuration. The martensite variants are described by the gradient tensor $\nabla \boldsymbol{y} = [(\partial y_i/\partial x_j)]$, which can assume one of the three forms:

$$U_1 = \begin{pmatrix} \eta^2 & 0 & 0 \\ 0 & 1/\eta & 0 \\ 0 & 0 & 1/\eta \end{pmatrix}, \qquad U_2 = \begin{pmatrix} 1/\eta & 0 & 0 \\ 0 & \eta^2 & 0 \\ 0 & 0 & 1/\eta \end{pmatrix},$$
$$U_3 = \begin{pmatrix} 1/\eta & 0 & 0 \\ 0 & 1/\eta & 0 \\ 0 & 0 & \eta^2 \end{pmatrix}, \tag{1}$$

for a uniaxial volume-conserving stretch along the three cartesian axes. The set of energy-minimizing states consists of all possible rotations of the three deformation variants, and can be written as

$$K = \bigcup_{i=1}^{3} \mathrm{SO}(3) U_i, \tag{2}$$

where SO(3) denotes the group of three-dimensional proper orthogonal transformations (rotations).

Similarly, smectics can be described by a scalar displacement field $\phi = \phi(\boldsymbol{x})$, which measures the local displacements from a set of flat equally spaced surfaces. The smectic layers are equipotential surfaces of ϕ, with the layer normals $\boldsymbol{N} = \boldsymbol{N}(\boldsymbol{x}) \equiv -\nabla\phi$. Note that the displacement field defines a surface with constant slope ($|\nabla\phi| = 1$) in the four-dimensional "space-time" ($\{\phi, x, y, z\}$)—forming "light surfaces" in the order parameter field (see Ref. [15]). This analogy to special relativity, and the Lorentz invariance of the allowed smectic domains, will be central to our proposed martensitic analysis of 3D smectic layers.

The Dupin cyclides may be defined as the surfaces whose centers of curvatures lie along one-dimensional curves. Since the condition of equally spaced layers ($N^2 \equiv 1$) implies that the centers of curvature are shared by subsequent surfaces, a domain filled with Dupin cyclides allows the system to form relatively cheap line singularities, rather than the energetically expensive two-dimensional singular centers of curvature of typical curved surfaces. The geometry of the Dupin cyclides furthermore forces the singular curves to be conic sections—generically ellipses and hyperbolas passing perpendicularly through one another's foci.

Before analyzing 3D smectic domains, let us analyze a simpler case: smectic layers at a flat interface, where the layers are constrained to approach perpendicular to the boundary. Such *planar* boundary conditions are often found at surfaces like glass slides; they are called planar because the smectic molecules (normal to the layers) are in the plane of the boundary surface. Figure 3 shows the displacement field ϕ (top grey surface) and some layers (bottom black lines) as a function of x and y at the top

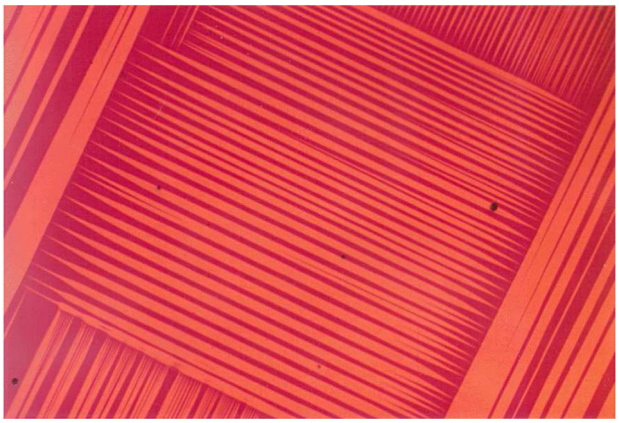

FIG. 2. Experimental martensitic microstructure. Different variants (colors) U_i can rotate via an SO(3) symmetry so as to join together compatibly at twin boundaries. Courtesy of Chu and James [14].

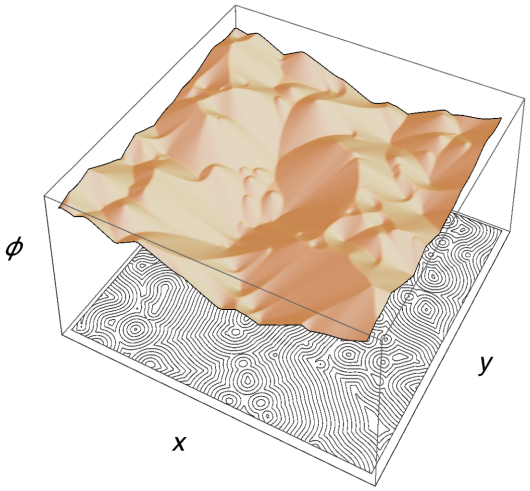

FIG. 3. Displacement field ϕ (top grey surface) and some of its levels (bottom black lines) as a function of x and y for the top planar boundary of a simulated configuration of smectic liquid crystals. Note that each domain of concentric circles on the bottom becomes a positive or negative light cone in the surface defining $\phi(x, y)$.

(planar) boundary of a smectic configuration (the same used in Fig. 1). At a planar boundary, the cyclides of Dupin form concentric circles [Fig. 1(c)], corresponding to "light cones" in the figure with space-time centers $\{\phi_0, x_0, y_0\}$. The corresponding displacement fields can be described in terms of two variants

$$U^{(2)}_{\pm}: \phi = \pm\sqrt{x^2 + y^2} \tag{3}$$

together with the three-dimensional group of translation operations (two translations in space and one in time)

$$T(3): \{\phi, x, y\} \to \{\phi - \phi_0, x - x_0, y - y_0\} \tag{4}$$

leading to a space of low energy structures

$$K^{(2)} = \bigcup_{\alpha=\pm} T(3) U^{(2)}_{\alpha}. \tag{5}$$

In the full three-dimensional smectic domains, we may not only translate and rotate the Dupin cyclide domains, but we may also transform them under dilatations and Lorentz boosts (which change the eccentricity of the ellipses and hyperbolas [15], leading [16] to the Weyl-Poincaré group $\mathcal{WP}$ [17]. This group, which is a semidirect product of positive dilatations and Poincaré transformations, is an 11-dimensional group. We can form a general Dupin domain by the action of 9 generators of $\mathcal{WP}$ (which correspond to the quotient of $\mathcal{WP}$ by a 2D Abelian subgroup) on a toroidal domain, whose singular curves are a unit circle in the xy plane and a perpendicular line through its center (see Sec. II in Supplemental Material) [18]. Since this domain is the product of two cones, $[(r+1)^2+z^2-\phi^2][(r-1)^2+z^2-\phi^2]=0$, with $r=\sqrt{x^2+y^2}$, there are four variants now [19],

$$U^{(3)}_{\pm\pm}: \phi = \pm\sqrt{(r \pm 1)^2 + z^2}, \tag{6}$$

hence leading to a huge space of low energy structures

$$K^{(3)} = \bigcup_{\alpha,\beta=\pm} \mathcal{WP} U^{(3)}_{\alpha\beta}. \tag{7}$$

We employ numerical simulations to generate the smectic configurations that are used in our microstructure analysis. Our simulations describe the dynamical evolution of the layer normal field $\boldsymbol{N} = \boldsymbol{N}(\boldsymbol{r})$ along the gradient-descent path of an elastic free energy [5]. We consider the following adaptation of the Oseen-Frank free-energy functional [20–22]:

$$F_s = \int d\boldsymbol{r}[f_s(\boldsymbol{N}, \nabla\boldsymbol{N}) + \boldsymbol{\lambda} \cdot \nabla \times \boldsymbol{N}], \tag{8}$$

with the energy density f_s given by

$$f_s = \frac{B}{4}(1 - N^4)^2 + KN^2(\nabla \cdot \boldsymbol{N})^2 + \frac{1}{2}K_{24}N^2\nabla \cdot [(\boldsymbol{N} \cdot \nabla)\boldsymbol{N} - \boldsymbol{N}(\nabla \cdot \boldsymbol{N})], \tag{9}$$

where B, K, and K_{24} are constants. The first term in Eq. (9) is a compression term, which penalizes elastic distortions of the smectic interlayer spacing. The second and third terms are related to the usual splay and saddle-splay distortions [1]. Notice the unusual amplitude dependence ($\sim N^2$) multiplying the K and K_{24} elastic terms. It originates in gradient distortions of the form $(\nabla Q)^2$, which are proportional to N^2 for nematic uniaxial ordering [5,23], where $Q = [(Q_{ij})]$ is the Maier-Saupe tensorial order parameter. We also use a Lagrange multiplier $\boldsymbol{\lambda}$ to forbid the existence of dislocations. The layer-normal field $\boldsymbol{N}$ satisfies the set of partial differential equations:

$$\gamma\dot{\boldsymbol{N}} = -\left(\frac{\delta F_s}{\delta \boldsymbol{N}} - \left\langle \frac{\delta F_s}{\delta \boldsymbol{N}} \right\rangle\right), \tag{10}$$

where the angle brackets denote a spatial average and γ is a viscosity constant. The second term of Eq. (10) ensures that the net number of layers in the cell does not change during a gradient descent step. Initially, we generate a random order parameter field $\boldsymbol{N}$, and use a Euler integrator with adaptive control system to solve the set of PDEs given by Eq. (10). We consider a cubic grid with global tetragonal shape of size $256 \times 256 \times 64$. The elastic constants are fixed so that de Gennes's length scale $\xi \equiv \sqrt{K/B} = 0.2a$, and $K/K_{24} = -1.5$, where a is the simulation lattice spacing. In

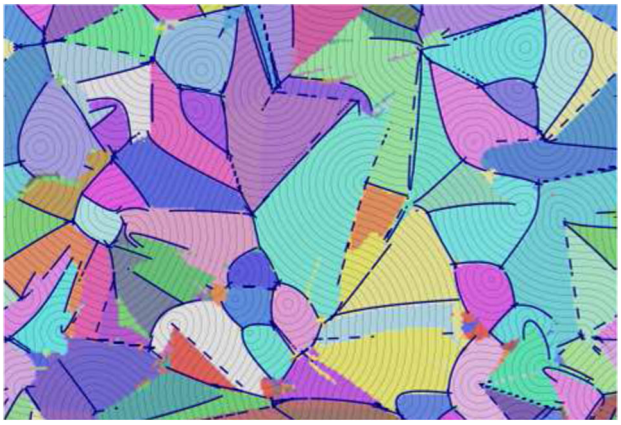

FIG. 4. Smectic microstructure of a two-dimensional planar boundary of a 3D simulation. The intersection of smectic layers and the section form sets of concentric circles, which are shown as thin black curves. The boundary between clusters (blue lines) are conics satisfying suitable compatibility conditions. Straight dashed lines separate domains whose "light cones" are pointed in opposite directions and just miss tangency.

the present paper, we only consider planar anchoring with the top and bottom boundaries; i.e., we fix $N_z = 0$ at $z = 0$ and $z = L_z$. Our code combines the versatility of Python with fast parallel programming using CUDA. To obtain the configuration displayed in Figs. 1, 3, and 4, we evolved $\boldsymbol{N}$ for a total time $t_t \approx 2,000\gamma/B$ [24]. More details of the simulations can be found in [5].

We developed a clustering algorithm to decompose smectic planar sections into domains with distinct centers, i.e. the low-energy structures described in Eqs. (3)–(5). For each domain (we start with square clusters), we use a least-squares optimization algorithm to find the four-tuple $X_\alpha = (\phi_{0,\alpha}, x_{0,\alpha}, y_{0,\alpha}, \sigma_{0,\alpha})$ that minimizes the cost function (see Supplemental Material [18])

$$C_\alpha = \sum_i c(r_{i,\alpha}, X_\alpha), \tag{11}$$

where the sum runs over points in $(2+1)$D space that belong to cluster α, and

$$c(r_i, X_\alpha) = \{\phi_i - \phi_{0,\alpha} + \sigma_{0,\alpha}[(x_i - x_{0,\alpha})^2 + (y_i - y_{0,\alpha})^2]^{1/2}\}^2 + \left(N_x - \frac{x_i - x_{0,\alpha}}{d_{i0,\alpha}}\right)^2 + \left(N_y - \frac{y_i - y_{0,\alpha}}{d_{i0,\alpha}}\right)^2, \tag{12}$$

where $d_{i0,\alpha} = [(x_i - x_{0,\alpha})^2 + (y_i - y_{0,\alpha})^2]^{1/2}$ is the 2D Euclidean distance from point i to the center, and $\sigma_{0,\alpha} = \pm 1$ characterizes the nappe of the cone [25]. By minimizing the first term on the right-hand side of Eq. (12), we find the best approximation for the local energy minimizer in the set (5). The second and third terms make the analysis sensitive to gradient changes. The next step is to redefine the clusters so that each pixel in $(2+1)$D space is associated with the center that yields the least cost $c(r_i, X_\alpha)$. This entire process is iterated several times. At the end, we merge a few clusters that are described by similar parameters X_α. Figure 4 shows a plot of our cluster decomposition, where each pixel is colored according to the cluster centers X_α.

The colored regions in Fig. 4 are analogous to the martensitic domains in Fig. 2. Note the elliptical domains (just lower left of center) are only a small fraction of the total area; as in many experiments, much of the region is not an Apollonian packing of focal conic domains (and hence not described by Friedel's laws of association). The nonelliptical domains nonetheless appear to be filled with cyclides of Dupin.

Finally, we turn to the compatibility conditions. In our example of martensites [Eqs. (2) and (1)], the constraint that the field $\mathbf{y}(\mathbf{x})$ is continuous forces the boundaries between variants to be rotated by specific angles: if $\nabla \mathbf{y} = K_1 = R_1 U_i$ and $K_2 = R_2 U_j$ are to meet continuously along a twin boundary (the boundaries between the lamellae in Fig. 2), then $K_1 - K_2$ must be zero along the boundary.

What are the compatibility conditions for our smectic concentric sphere domains at the planar boundary, allowing $\phi(\mathbf{y})$ to be continuous? Compatible boundaries between domains of concentric circles are the projections of the intersection of two conic surfaces onto the xy plane. We can find the singular conic solutions by solving the pair of equations:

$$(x - x_0)^2 + (y - y_0)^2 - (\phi - \phi_0)^2 = (x - x_1)^2 + (y - y_1)^2 - (\phi - \phi_1)^2, \tag{13}$$

$$(x - x_0)^2 + (y - y_0)^2 - (\phi - \phi_0)^2 = 0, \tag{14}$$

for x and y. This algebraic manipulation results in the smectic compatibility equation:

$$(x - x_0)^2 + (y - y_0)^2 = [x_0^2 - x_1^2 - 2x(x_0 - x_1) + y_0^2 - y_1^2 - 2y(y_0 - y_1) + (\phi_0 - \phi_1)^2]^2 / [4(\phi_0 - \phi_1)^2], \tag{15}$$

a quadratic equation whose solutions are conic sections in the boundary surface dividing neighboring smectic domains. The dark lines in Fig. 4 show compatible boundaries in the smectic microstructure given by the ellipses and hyperbolas of Eq. (15).

We conjecture that the compatibility condition for 3D smectic domains will lead to boundaries, as described by Friedel [8], which are portions of right circular cones connecting one point of a conic to its confocal partner.

How have we altered the standard theory of martensites? First, our elastic free energy density is written in terms of the gradients of N, and hence *second* derivatives of the displacement field ϕ—a strain gradient theory. Second, our domains are not described by a uniform deformation but

rather by a deformation determined by the nonlocal constraints [26] imposed by the constraint of one-dimensional singularities. Conversely, what further can we glean from the martensitic analogy? The mathematical engineers use sophisticated real analysis (minimizing sequences and Young measure distributions) to describe the family of boundary conditions that can be relaxed by an infinitely fine microstructure [10–12]. Apollonian microstructures formed by a hierarchy of ellipses are known to mediate smectic tilt boundaries [7,27,28]. An infinitely fine laminate of alternating concentric spheres and Dupin domains, inspired by the experimental "flower texture," has been shown to relax an arbitrary cylindrically symmetric boundary condition [13]. But the general question remains a fascinating one: what is the class of smectic boundary conditions that can be mediated by structures of equally spaced layers with only line singularities?

We would like to thank R. D. James for useful conversations. D. B. L. acknowledges the financial support provided by the Brazilian agency Capes. This work was supported in part by the Department of Energy DOE-BES DE-FG02-07ER46393 (J. P. S., M. K. B., and D. B. L.) and by a Simons Investigator grant from the Simons Foundation to R. D. K. R. A. M. and R. D. K. were supported through NSF Grant No. DMR12-62047. R. A. M. acknowledges financial support from FAPESP Grant No. 2013/09357-9.

*dl778@cornell.edu
†sethna@lassp.cornell.edu

[1] P. G. de Gennes and J. Prost, *The Physics of Liquid Crystals* (Claredon Press, Oxford, 1993).
[2] In this paper we ignore thermal fluctuations, which in three-dimensional smectic liquid crystals destroy the long-range translational order (leading to power-law correlations in the density-density correlation function perpendicular to the layers). See P. M. Chaikin and T. C. Lubensky, *Principles of Condensed Matter Physics* (Cambridge University Press, Cambridge, England, 1995).
[3] G. Friedel and F. Grandjean, Bull. Soc. Franc. Minér. **32**, 192 (1910).
[4] Simulated crossed-polarizer images are produced via the calculation of the transmitted intensity of scattered light going through the anisotropic liquid-crystalline medium (see, e.g., [1,7]). To mimic focused images in the top slide of a smectic sample, we render a density plot with the gray scale corresponding to the scattering amplitude $N_x N_y$ at the top-layer section of a simulation. The layer surfaces in Fig 1(c) can be obtained by solving the equation $\boldsymbol{N} = \nabla\phi$ for ϕ, using Fourier methods. More information on our smectic visualizers can be found in our previous publication [5].
[5] D. B. Liarte, M. Bierbaum, M. Zhang, B. D. Leahy, I. Cohen, and J. P. Sethna, Phys. Rev. E **92**, 062511 (2015).
[6] D. Hilbert and S. Cohn-Vossen, *Geometry and Imagination* (AMS Chelsea Publishing, Providence, RI, 1999).
[7] M. Kleman and O. D. Lavrentovich, *Soft Matter Physics: An Introduction* (Springer-Verlag, New York, 2003).
[8] G. Friedel, Ann. Phys. (Paris) **18**, 273 (1922).
[9] K. Bhattacharya, *Microstructure of Martensite: Why it forms and how it gives rise to the shape-memory effect* (Oxford University Press, Oxford, 2003).
[10] J. M. Ball and R. D. James, Arch. Ration. Mech. Anal. **100**, 13 (1987).
[11] J. M. Ball and R. D. James, Phil. Trans. R. Soc. A **338**, 389 (1992).
[12] J. M. Ball, Mater. Sci. Eng. A **378**, 61 (2004).
[13] D. A. Beller, M. A. Gharbi, A. Honglawan, K. J. Stebe, S. Yang, and R. D. Kamien, Phys. Rev. X **3**, 041026 (2013).
[14] C. Chu, Ph.D. thesis, University of Minnesota, 1993.
[15] G. P. Alexander, Bryan Gin-ge. G. Chen, E. A. Matsumoto, and R. D. Kamien, Phys. Rev. Lett. **104**, 257802 (2010).
[16] G. P. Alexander, R. D. Kamien, and R. A. Mosna, Phys. Rev. E **85**, 050701(R) (2012).
[17] J. Bertrand and P. Bertrand, in *Wavelets*, edited by J.-M. Combes, A. Grossmann, and P. Tchamitchian (Springer Berlin Heidelberg, 1990), pp. 232–238.
[18] See Supplemental Material at http://link.aps.org/supplemental/10.1103/PhysRevLett.116.147802 for a brief introduction to the mathematical theory of martensites, an expansion of the argument for the four-dimensional low-energy structures of smectics, and additional details on our numerical domain decomposition.
[19] The two extra choices for the sign correspond to setting $(r-1)^2 + z^2 - \phi^2 = 0$ or $(r+1)^2 + z^2 - \phi^2 = 0$ in the equation for the toroidal FCD (see main text). In the first case we obtain Dupin surfaces formed by regions with both positive and negative Gaussian curvature; the FCD of the first species corresponds to the negatively curved regions. In the second case we obtain the FCD of the second species, for which only the hyperbola is visible under the microscope (the ellipse being virtual) [7].
[20] C. W. Oseen, Trans. Faraday Soc. **29**, 883 (1933).
[21] H. Zocher, Trans. Faraday Soc. **29**, 945 (1933).
[22] F. C. Frank, Discuss. Faraday Soc. **25**, 19 (1958).
[23] D. C. Wright and N. D. Mermin, Rev. Mod. Phys. **61**, 385 (1989).
[24] In our simulations, the coarsening of FCDs does not stop until a flat configuration is reached (though it becomes very slow at later times). We have also applied our methodology to later configurations, which display larger and simpler features, but no essential qualitative changes. As discussed in [5], we are able to stabilize defect structures by simulating "dust" particles on the boundaries.
[25] The "nappe" of a double cone is the conic region above *or* below the cone apex.
[26] J. P. Sethna and M. Kleman, Phys. Rev. A **26**, 3037 (1982).
[27] M. Kleman and O. D. Lavrentovich, Eur. Phys. J. E **2**, 47 (2000).
[28] R. Bideaux, N. Boccara, G. Sarma, L. de Sèze, P. G. de Gennes, and O. Parodi, J. Phys. **34**, 661 (1973).